Analogue Wireless Beamforming Exploiting the Fiber-Nonlinearity of Radio Over Fiber Based C-RANs

Yichuan Li, *Student Member, IEEE*, Salman Ghafoor, K. Satyanarayana, *Student Member, IEEE*, Mohammed El-Hajjar, *Senior Member, IEEE*, Lajos Hanzo, *Fellow, IEEE*

***Abstract*—As a key technique of supporting the fixed backbone network, radio over fiber (RoF) systems transmit the radio frequency signals over optical fiber in order to take advantage of their large available bandwidth. In this context, optical fiber aided phased antenna array (PAA) based beamforming techniques have attracted substantial research interest with the goal of improving the cell-edge coverage of cellular base stations. In this paper, we conceive a novel optical fiber aided beamforming technique based on the fiber's nonlinearity to be applied in cloud radio access network (C-RAN). In our proposed technique, the PAA elements are fed by the phase-shifted signals introduced by our highly nonlinear fiber (HNLF) aided phase-shifting solution, which results in an angular beamsteering range of around 90°. This can be exploited by sectorization in cellular networks to reduce the cochannel interference imposed. Furthermore, we exploit the proposed RoF-aided phase shifting technique in C-RAN, where our proposed system takes advantage of the centralized signal processing capability of the RoF system to conceive an all-optical processing based tunable beamforming system. While our flexible HNLF-aided phase-shifting process is confined to the central office of the C-RAN, the end users in the C-RAN cellular networks are capable of flexibly choosing the serving remote radio heads (RRHs) and employing diverse wireless transmission techniques. Through integrating our HNLF-aided phase-shifting design into the proposed C-RAN, we impose as little as 0.1 dB signal-to-noise Ratio (SNR) degradation compared to its traditional electronic counterpart, which requires extra phase-shifters.**

Index terms Optical fiber, C-RAN, phased array antenna beamforming, phase-shifter, optical nonlinearity, self-phase modulation, cross-phase modulation, highly nonlinear fiber.

I. Introduction

Next generation networks require an ever-increasing capacity [1]. The small cells of the emerging dense networks are expected to support more users [2]. In this context, beamforming techniques relying on phased antenna arrays (PAA) [3], which steer the signal beams in a desired direction are widely used for cell-sectorization. It constitutes a promising application of the emerging large-scale multiple-input-multiple-output (MIMO) system relying on numerous antennas, owing to their high power efficiency, excellent cell-edge coverage and reduced co-channel interference in cellular network [4].

On the other hand, we invoke a cloud radio access network (C-RAN) [5], [6], where a central office housing the centralized baseband signal processing [7] serves multiple low-complexity and low-cost remote radio heads (RRHs). The proposed C-RAN [8] invokes Radio over Fiber (RoF) [9] transmissions to the RRHs for supporting the emerging small-cell technologies [8].

Furthermore, the fiber-based C-RAN fronthaul has been widely advocated for employment in future wireless networks as a benefit of the fiber's high capacity, low attenuation, immunity to electromagnetic interference, etc [10], [11]. In this context, it is beneficial to investigate the feasibility of using optical fiber to assist beamforming by circumventing the employment of a large number of electronic Radio Frequency (RF) phase-shifters, which have a high insertion loss.

Figure 1 shows an optical fiber aided beamforming system, which utilizes an optical fiber based delay line for a centralized controlled beamforming scheme. These optical fiber aided beamforming solutions have several benefits compared to the traditional RF solutions in the context of beamforming, which are listed as follows:

1) Using the optical fiber, fiber based fronthaul networks can share the optical transmitter or optical receiver, requiring no additional components for up/down-conversion.
2) The low-complexity RoF network design aims for reducing the complexity by exploiting the fiber's properties-induced phase-shift for beamsteering, hence eliminating any additional processing, which would otherwise be required for carrying out the beamforming-specific phase shift.
3) A lower insertion loss is imposed by a fiber-based phase-shifter compared to its electronic counterpart [12].

The fiber aided beamforming technique has grown in popularity in recent years [13]–[18]. The beamforming techniques based on the Fiber Bragg Grating (FBG) utilize a number of uniform FBGs [13]–[15] or a single tunable linear chirped FBG [16]–[18]. Furthermore, other fiber-based beamforming techniques, such as a dispersive switched fiber delay line to obtain the desired time delay corresponding to the specific phase-response have also been investigated [19]. Other solutions, such as optical demultiplexing relying on a specific configuration of multiple ports [20], on photonic crystal fibers [3], on optical ring resonators [21], and on spatial light modulators [22] have also been researched.

The financial support of the EPSRC projects EP/Noo4558/1 and EP/L018659/1, as well as of the European Research Council's Advanced Fellow Grant under the Beam-Me-Up project and of the Royal Society's Wolfson Research Merit Award is gratefully acknowledged. Copyright (c) 2015 IEEE. Personal use of this material is permitted. However, permission to use this material for any other purposes must be obtained from the IEEE by sending a request to pubs-permissions@ieee.org.

Y. Li, K. Satyanarayana, M. El-Hajjar, and L. Hanzo are with the School of ECS, University of Southampton, SO17 1BJ, United Kingdom (e-mail: yl2e13@ecs.soton.ac.uk; meh@ecs.soton.ac.uk; lh@ecs.soton.ac.uk).

S. Ghafoor is with the National University of Sciences and Technology, Pakistan (e-mail: salman.ghafoor@seecs.edu.pk).

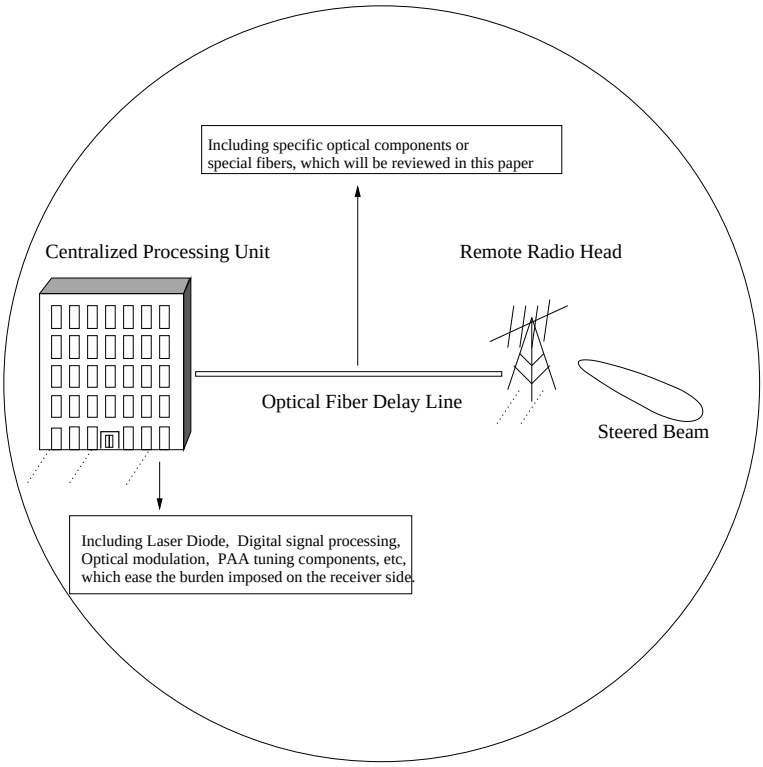


Figure 1: Basic Concept of Optical Fiber Aided Beamforming.

In a nutshell, the FBG-based technique is a scalable solution, which exhibits flexible tunability, low loss, short fiber length and a low-complexity system configuration. However, the phase inaccuracy resulting from the group delay ripple caused by the fabrication of the FBG [23] for example is a key issue to be further researched.

As alluded to above, nonlinear fibers may be characterized by their specific phase responses [24], while exploiting the harmful fiber-nonlinearity for PAA beamforming. In [25], a photonic phase-shifter based on stimulated Brilloin scattering was proposed, which requires a table pump source in order to control the phase shift of the output to be fed into the PAA elements. By contrast, in [26] a phase-shifter based on cross-phase modulation was illustrated. In [27], a phase-shifter based on the nonlinear polarisation rotation imposed by an HNLF was invoked for the PAAs. However, requiring an excessive number of phase-shifters for realizing a highly directional beamforming pattern makes the techniques reported in [25]–[27] somewhat impractical. *As a compelling proposition, we jointly design the nonlinearity of the optical fiber and a power control unit so that a linear phase response is constructed from the carefully conceived combination of Self-Phase Modulation (SPM) and Cross-Phase Modulation (XPM).*

The fundamental objective of our proposed technique is to take advantage of the phase shift imposed by SPM and XPM, where the nonlinearity-induced phase shift caused by SPM and XPM is highly dependent on the power profile of the optical source. After transmission through a short parallel HNLF, the optical signal is then fed into a dispersion-shifted fiber (DSF) for data transmission, which exibits low dispersion in our wavelength region [28]. Then, the received optical signal is converted to the corresponding phase-shifted RF signal, after which a set of signals subjected to linear phase shift is extracted by a filter and fed into the PAA elements. *To the best of our knowledge, this is the first time that HNLF transmission line based technique is conceived for supporting tunable phase-shifting using SPM and XPM, hence substantially simplifying the photonic phase-shifting arrangement required.* The proposed technique achieves a beamsteering angular range of about 90°, which we invoke for sectorization. This range can be readily extended to 360° by either using longer HNLFs or by specific fibers exhibiting higher nonlinearity[1]. Furthermore, as an application of our HNLF-based phase-shifting beamforming system, a C-RAN network exploiting our design is analyzed, where the end users may connect to one or several RRHs, depending on the channel conditions.

In this paper, we propose employing an HNLF transmission line, which exploits the XPM-SPM-induced phase shifts to build a RoF aided beamforming system. The beam steering is carried out in the optical domain using a centralized processing unit. Compared to the previously proposed fiber-aided beamforming techniques, the advantages of our design using HNLF and the novel contributions of this paper can be summarized as follows:

1) We conceive for the first time a beamformer relying on short parallel HNLF lines, which forms a centrally controlled beamforming system designed for the C-RAN fronthaul of low-cost small-cell networks. Meanwhile, the BER performance of the proposed system is main-

[1]Using a longer fiber or a fiber with higher nonlinearity factor, it is possible to extend the coverage angle of the antenna array in each RRH to 360°. In this example proposed, where the coverage angle is 90°, it is possible to employ four antenna arrays at the same RRH, where each antenna array can cover a different 90° area and hence the RRH will be able to cover the entire 360° area.

tained in comparison with that of the electronic phase-shifter aided beamforming schemes.
2) A tunable HNLF transmission line based on jointly harnessing the SPM and XPM has never been used for beamforming before. Explicitly, we exploit the unavoidable fiber-nonlinearity for phase-shifting-based beamforming, instead of relying on conventional extra phase-shifters.
3) We present a design example using four antenna elements. However, our solution is not limited to the design example employing four antenna elements in Section II. Explicitly, it allows us to increase the number of wavelengths and to employ shorter HNLFs in order to increase the PAA's angular selectivity, making it flexibly scalable.
4) We transmit a quadrature-phase-shift-keying (QPSK) signal at 10 Gbps data rate as an example for demonstrating that our design can be employed in the C-RAN designed in [29], where non-line-of-sight (NLOS) wireless communication is applied.

The rest of the paper is organized as follows. In Section II, the system model of our all-optical phase shifting technique and its application in a C-RAN system are presented. Then, our simulation results and analysis are discussed in Section III, followed by our conclusions in Section IV.

II. Proposed System Model

In this section we propose a phase-shifter based PAA aided beamforming system using HNLF and investigate its benefits in the C-RAN system proposed in [29], resulting in a low-complexity scalable system configuration relying on centralized signal processing. Our system exploits the power-controlled fiber-nonlinearity-induced phase shifts, where the phase shift of each antenna element of Figure 2 is controllable through a programmable optical attenuator in a centralized processing unit at the input of the fiber, which significantly reduces the complexity imposed on the RRHs at the fiber's output. Note that our proposed design is applicable to cellular sectorization scenarios, for example for a a sector range of 90° [30]. To the best of our knowledge, HNLF parallel transmission line based phase shifting has not been used for MIMO beamforming before.

A. System Overview

Figure 2 shows the block diagram of our proposed beamformer utilizing both HNLF and wavelength evolution in each step. Assuming that only a single wavelength λ_1 is transmitted in this system, the associated wavelength landscape-evolution displayed in Figure 2. Then, the wavelength having the designed power is modulated by a MZM modulator to obtain an optical single side-band signal. Afterwards, the modulated signal is injected into a short HNLF having a length below 1 km along with a control signal generated by the LD of Figure 2. A power-dependent phase-shift is imposed and tuned by the XPM induced by the control signal, whose power is tuned by a controllable optical attenuator, as shown in Figure 2. Then, the output power of the HNLF will be fed into the DSF, where the zero-dispersion wavelength is shifted to the vicinity of 1550 nm [28] for transmission to a remote radio port. The phase is then retained after coherently photo-detecting the RF signal. Thus, based on the power-dependent phase shift of the wavelength transmitted in the HNLF which will be detailed in Section II-A1, the power controller will adjust the power level of the control signal for adjusting the corresponding phase shift.

Relying on the above discussions related to the conception of a tunable phase-shifting aided beamforming system, our design philosophy is now extended to the tunable multi-wavelength source seen in Figure 2 and using four wavelengths as a design example [2]. Then, the multi-wavelength source injects the optical signal into a MZM to generate a optical single side band (OSSB) signal driven by a Binary Phase Shift Keying (BPSK) modulated electronic signal. As seen at the bottom of Figure 2, four optical attenuators are used for tuning the power of the four individual control signals fed into each HNLFs. The HNLF is used for imposing different phase shifts for each wavelength due to the XPM induced by the control signal, as detailed below. After transmission through the HNLF, a wavelength multiplexer combines the optical signal into a Wavelength Division Multiplexing (WDM) signal of λ_1 λ_2 λ_3 λ_4 for feeding it into a DSF, where the zero-dispersion wavelength is in the vicinity of 1550 nm. The WDM signal is then split into four branches by a demultiplexer in the example of Figure 2. Then each branch is fed into a coherent photo detector (PD) for converting the optical signal to an RF signal, which is fed into an electronic amplifier. Finally, the amplified RF signal is fed into each antenna at the same power level for ensuring a satisfactory directivity. In other words, each output of the electronic amplifier feeds a PAA element employing uniform linear arrays, with each element being fed by linearly delayed RF signals. This allows the scheme to steer the RF signal in the desired direction, which is an explicit benefit of combining the appropriately phased signals fed into the antenna elements. Finally, corresponding to the specific locations of the mobile users, the beamsteering angle can be controlled by the specific phase-shift between the adjacent antenna elements.

Next, we provide our simulation-based results to verify our proposed design. Generally, the signal transmitted through the optical fiber suffers from fiber attenuation, fiber dispersion and fiber nonlinearity [28], [31]. The fiber attenuation causes power-loss, while the fiber dispersion imposes both pulse broadening and inter-symbol-interference. Fiber nonlinearity engenders Stimulated Brillouin Scattering (SBS), Stimulated Raman Scattering (SRS), SPM, XPM and Four-Wave-Mixing (FWM), which yield frequency chirping and phase shifting. These effects are routinely considered in fiber-optic communication systems. However, in our system, the SRS, SBS and FWM can be neglected due to having a low optical input power and phase-mismatch [31], which will be elaborated on in the next section.

Thus, considering the fiber impairments above, the mathematical principle of the HNLF channel model based on the Symmetric Split Fourier Method (SSFM) with XPM and SPM will be presented.

[2]For lager size of MIMO system, we need more wavelengths and more short HNLF, but this can be readily realized by tuning multi-wavelength laser source and increasing the number of the deployed short HNLFs.

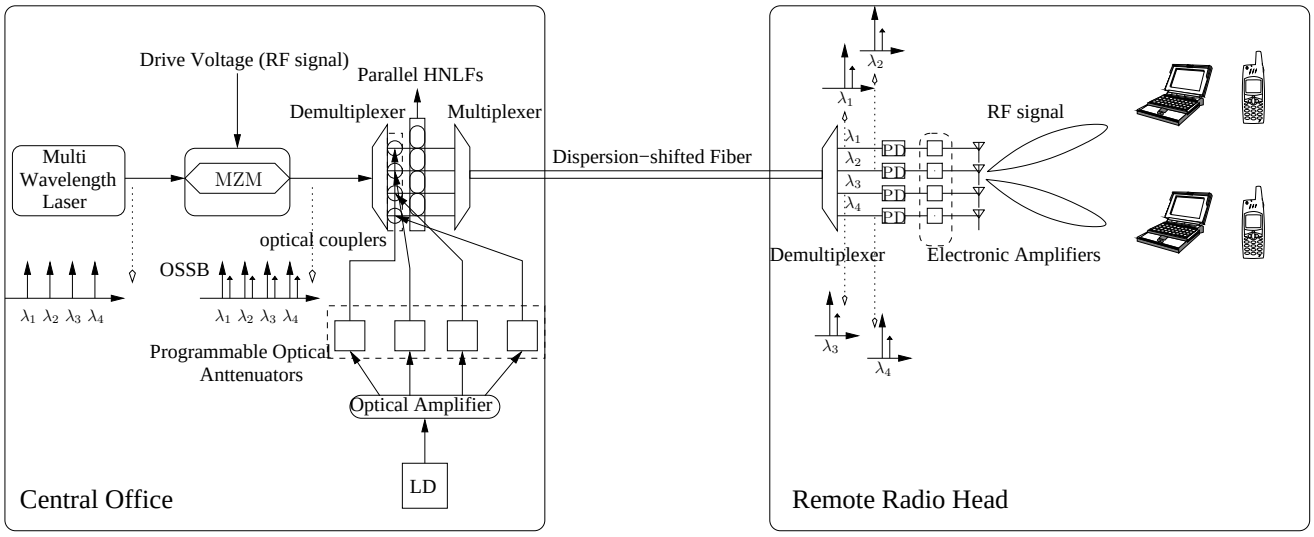


Figure 2: Schematic of a four-element beamformer based on HNLF-RoF system.

1) Symmetric Split-step Fourier Method with XPM and SPM: The SSFM is widely used in single-mode fiber (SMF) simulations both for pulse based signals [31] and for continuous wave transmission [31].

To study the impact of SPM and XPM, a simplified form of the nonlinear Schrödinger equation is used [31]:

$$i\frac{\partial A}{\partial z} + \frac{i\alpha}{2}A - \frac{\beta_2}{2}\frac{\partial^2 A}{\partial t^2} + \gamma|A|^2 A = 0, \tag{1}$$

where A is the amplitude of the optical input signal, z is the fiber length, α denotes the fiber loss, β_2 is the second order dispersion parameter, which accounts for the chromatic dispersion and γ is the nonlinearity parameter [32]. Upon taking into account the impact of SPM first, based on the SSFM, we arrive at [31]:

$$\frac{\partial A}{\partial z} = (\hat{D} + \hat{N})A, \tag{2}$$

where $\hat{D}$ is a differential operator that represents both the fiber loss as well as the dispersion and $\hat{N}$ is the nonlinearity operator representing the SPM. Combining Equations (1) and (2), yields:

$$\hat{D} = -\frac{\alpha}{2} - \frac{i\beta_2}{2}\frac{\partial^2}{\partial t^2}, \tag{3}$$

$$\hat{N} = i\gamma|A|^2. \tag{4}$$

To elaborate briefly, the SSFM splits the fiber into numerous short segments of length h, over which the fiber may be deemed linear. There are three operations for each step, in which the first and third step represent the linear operations calculating the attenuation and dispersion, while the second operation represents the nonlinear operations. The first operation occurs in the first half interval of length $h/2$ and can be described as:

$$A(\omega, z + \frac{h}{2}) = exp[\frac{h}{2}\hat{D}(i\omega)]A(\omega, z), \tag{5}$$

where $A(\omega, z + \frac{h}{2})$ is the Fourier transform of $A(t, z + \frac{h}{2})$ and the differential operator $\partial/\partial t$ is replaced here by $i\omega$. Then, for the second operation taking place during the middle of the step, the nonlinearity would be accounted for as follows [31]:

$$A'(t, z + \frac{h}{2}) = A(t, z + \frac{h}{2})exp(h\hat{N}), \tag{6}$$

where $A'(t, z+\frac{h}{2})$ is the input signal for the next half step after the nonlinear operation [31], [33]. Finally, the third operation, which occurs during the second half step repeats the first process. This procedure can be expressed as [31]:

$$A(t, z + h) = exp(\frac{h}{2}\hat{D})exp(h\hat{N})exp(\frac{h}{2}\hat{D})A(t, z). \tag{7}$$

Self-phase modulation occurs, when a single optical beam transmitted through the fiber. More specifically, the reason for the phase-shift caused by SPM is that in HNLF, a high-intensity optical signal may result in the optical Kerr effect [31], which changes the refractive index of the optical fiber. This results in slowing down the light beam propagation in the fiber. In contrast to the self-induced phase modulation occuring in a single channel, XPM is caused by having more than one optical beams [28]. Thus, the refractive index affecting the optical beam in HNLF is dependent both on the intensity of its own and those of others. The SSFM described above only handles the effects of SPM, while for characterizing the combination of XPM and SPM, Equation (4) should be modified as follows:

$$\hat{N} = i\gamma(|A_i|^2 + 2\sum_{k\neq i}|A_k|^2), \tag{8}$$

where A_i is the amplitude of the transmitted optical signal and A_k is that of the co-propagating optical signal. Obviously, from Equation (8), that the change of refractive index will be higher when XPM is encountered. Furthermore, Leibrich and Rosenkranz [33] conceived an efficient improvement of the SSFM subjected both to XPM and SPM, making it possible to reduce the required number of simulation steps by a factor of up to 20 without degrading the accuracy of the channel model. In our design, the Leibrich-Rosenkranz method is utilised for the simulation of the HNLF.

In PAA, the beamforming pattern is influenced by two factors: the radiation pattern, which is jointly determined

by the type of the radiation source and the array factor[3], which is dependent on external influences, such as the phase progression, number of elements and the carrier frequency [34]. Here, in order to simplify the analysis, an isotropic radiator transmitting in all directions is assumed. Thus, it is the array factor which predominately affects the beamforming angle. Explicitly, the array factor (AF) is expressed as [34]:

$$AF(\psi) = \frac{sin(M\psi/2)}{Msin(\psi/2)} \tag{9}$$

Then, ψ can be expressed from Equation (9) as:

$$\psi = kdcos(\theta) + \phi, \tag{10}$$

where θ is the beamsteering angle around the axis of the antenna array orientation, d is the constant distance between the adjacent antenna elements and ϕ is the corresponding phase shift. Furthermore, M is the number of beamforming antenna elements, while k is the wave number given as $k = 2\pi/\lambda_{RF}$ [35]. Therefore, in our proposed system, the phase shift ϕ is introduced by the fiber's nonlinearity as shown in Equation (7), which is exploited for adjusting the beamforming pattern determined by Equation (10).

Additionally, radio over fiber systems are affected by fiber attenuation, fiber dispersion and fiber nonlinearity. Hence, our channel model includes the effects of fiber attenuation, fiber dispersion and SPM-XPM-induced fiber nonlinearity are encountered, but that the SBS, SRS and FWM can be neglected. SBS and SRS may indeed significantly degrade the system by reflecting and shifting the transmitted wavelength, when a high optical power is imposed [28]. However, we can ignore these two effects, since the input power of the transmitted wavelength is kept as low as 0.1 mW. This is far below the threshold of the given HNLF, since the corresponding SRS threshold is approximately 270 mW and that of SBS is 42.5 mW based on the theoretical analysis of [28]. Furthermore, we also note that invoking the nonlinearity-inducing technique of Four-Wave Mixing (FWM) is not necessary due to the presence of phase mismatch in our system. This is because the effects of FWM only become significant, when the phase mismatch in the fiber vanishes [31]. Thus, as a benefit of conveniently controlling the chromatic dispersions for our HNLF, FWM can indeed be eliminated as a benefit of carefully tailoring the chromatic dispersion with the objective of avoiding the phase match of the transmitted wavelengths in our HNLF [36]. Thus, SPM and XPM constitute the main contributions to phase variations in the HNLFs in our design.

To validate the feasibility of our parallel HNLF-aided beamforming, we investigate its performance in the context of a C-RAN, where the central office houses the parallel HNLF-aided components of Figure 3 and the RRHs are connected to it using fibers. To elaborate further, we utilize two RRHs in Figure 3. Explicitly, a single-user C-RAN design relying on two RRHs is considered, where a pair of fibers is used for fronthaul access. In this scenario, the user may connect to either one or both RRHs to achieve beamforming or beamforming combined with either diversity or multiplexing gains, depending on the wireless channel quality.

[3]According to [34], the total field strength radiated by an antenna array is equal to that of a single element positioned at the origin of the array multiplied by a factor, which uniquely and unambiguously defines the array factor.

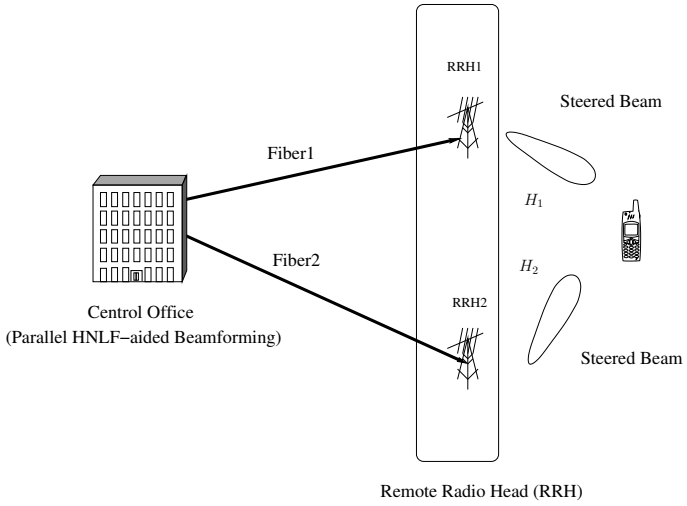


Figure 3: C-RAN beamforming System Model.

2) C-RAN System Model: In this section, we briefly describe the C-RAN system, which will be used for the verification of our HNLF aided PAA beamforming system, as shown in Figure 3. Beamforming substantially improves the SNR gain, thereby increasing the throughput [4]. Hence, instead of using phase-shifters for beamforming in the RRHs, we invoke the proposed all-optical processing based beamforming system, where HNLF aided phase shifting assisted beamforming is applied in Figure 3.

The C-RAN architecture can flexibly serve the end users in the cellular network [29], enabling them to achieve either diversity or multiplexing gains. As shown in Figure 3, the C-RAN fronthaul is fiber-based, where our HNLF aided PAA technique is employed for achieving beamforming, whilst simultaneously connecting the central office to the RRHs. Naturally the link between the RRH and the end-users is wireless.

In this C-RAN system, we adopt the approach of [29], where end-users may be connected to one or several RRHs, depending on the prevalent channel conditions, as follows.

1) If the wireless channels between the user equipment (UE) and both RRH1 as well as RRH2 of Figure 3 are favourable, then the UE may be connected to both RRH1 and RRH2, where either multiplexing or diversity gain is attained in addition to beamforming employed at each RRH.
2) On the other hand, when one of the wireless links is in deep fade, the UE is connected to only one of the RRHs, exploiting the better channel, thereby attaining an improved SNR [29]. In this case, the UE may be connected to either RRH1 or RRH2 of Figure 3.

In our design, we investigated both cases using our HNLF aided PAA beamforming technique for demonstrating the flexibility of our design. Thus, we integrated our HNLF-aided beamforming into a C-RAN system.

Let us now consider the network of Figure 3, where the user is equipped with N_r received antennas and each RRH is equipped with N_t transmit antennas. Furthermore, the user is positioned at an angle of ψ_1 and ψ_2 with respect to RRH1 and RRH2, respectively. In the scenario where the user is

connected to only one RRH, say RRH1, the received signal vector after combining is given by

$$\mathbf{y} = \beta \mathbf{w}^H \mathbf{H} \mathbf{f} x + \mathbf{w}^H \mathbf{n}, \tag{11}$$

where $\mathbf{f}$ is the beam steering vector of size $N_t \times 1$ formulated by the fiber, x is the input signal stream, $\mathbf{n}$ is the complex Gaussian noise of mean 0 and variance σ^2, $\mathbf{w}$ is the combining vector of size $N_r \times 1$, β is the RoF-system-induced distortion, while $\mathbf{H}$ is the semi-correlated channel with L paths, which is given by

$$\mathbf{H} = \sqrt{\frac{N_r N_t}{L}} \sum_{l}^{L} \alpha_l \mathbf{a}_r(\phi_r^l) \mathbf{a}_t^T(\phi_t^l), \tag{12}$$

so that $\mathbb{E}[\|\mathbf{H}\|_F^2] = N_t N_r$. Furthermore, $\mathbf{a}_r$ and $\mathbf{a}_t$ are the response vectors and for uniform linear arrays (ULA) they are expressed as:

$$\mathbf{a}_r(\phi_r) = [1 \; e^{j\frac{2\pi}{\lambda} d \cos(\phi_r)} \ldots e^{j\frac{2\pi}{\lambda}(N_r-1) d \cos(\phi_r)}]^T, \tag{13}$$

$$\mathbf{a}_t(\phi_t) = [1 \; e^{j\frac{2\pi}{\lambda} d \cos(\phi_t)} \ldots e^{j\frac{2\pi}{\lambda}(N_t-1) d \cos(\phi_t)}]^T, \tag{14}$$

where ϕ_r and ϕ_t are the angle of arrival and departure, respectively, while α_l is complex Gaussian distributed whose amplitude is Rayleigh and phase is uniformly distributed.

On the other hand, when the user is served by 2 RRHs, the signal vector received in the downlink is given by

$$\mathbf{y} = \beta \mathbf{W}^H \mathbf{H} \mathbf{F} \mathbf{x} + \mathbf{W}^H \mathbf{n}, \tag{15}$$

where $\mathbf{H}$ and $\mathbf{F}$ are now expressed as $\mathbf{H} = [\mathbf{H}_1 \quad \mathbf{H}_2]$ and $\mathbf{F} = \text{diag}\,(\mathbf{f}_1, \mathbf{f}_2)$, respectively. To elaborate further, $\mathbf{H}_i (i = 1, 2)$ is the sub-channel[4]matrix of size $N_r \times N_t$ of the link spanning from the i^{th} RRH to the UE as shown in Figure 3, while $\mathbf{f}_i (i = 1, 2)$ is the beam steering vector of size $N_t \times 1$ employed at the i^{th} RRH. The weights of the vector $\mathbf{f}_i$ are those of a zero-forcing beamformer, where the weights of the vector $\mathbf{f}_i$ is tuned for mitigating the interference caused by other RRHs, i.e. it can null the interference caused by a signal arriving from different angles. Furthermore, $\mathbf{x}$ is the signal vector of size 2×1, while $\mathbf{W}$ is now a matrix of size $N_r \times 2$. The signal transmitted by the beamforming at the RRHs is received by the UE, where the signal is downconverted and processed digitally in the baseband using the combiner matrix $\mathbf{W}^H$. In this paper, the linear minimum mean squared (LMMSE) solution[5] is chosen as the combiner matrix $\mathbf{W}^H$. This design can be interpreted as a sub-array architecture, which was depicted and discussed in great detail in [37]. A similar approach can be followed here for multiple RRHs association.

Next, our simulation results characterizing the power-controlled phase shifts are presented, while the system performance of Figure 3 is analyzed and compared to that of the system using traditional electronic phase-shifters without our Radio over Fiber aided beamforming.

III. Simulation Results and Discussions

In this section, we will first discuss the attainable phase shifts using our HNLF-aided beamforming scheme. Then, we characterize our fiber-based C-RAN system and benchmark it against that relying on traditional phase-shifters.

[4]It is instructive to note that, in this case, when two RRHs are used for transmission, $\mathbb{E}[\|\mathbf{H}\|_F^2] = 2N_t N_r$.

[5]Any combiner solution can be employed. We have considered LMMSE as a simplifying solution.

A. HNLF-aided Phase-shifting System

An HNLF channel transmitting QPSK modulated electronic signals of a multi-wavelength laser source has been simulated using MATLAB. The parameters used are shown in Table I.

More explicitly, a laser source having the four wavelengths of 1549.4, 1549.6, 1549.8 and 1550 nm is modulated by an RF signal having the centre frequency of 6 GHz, where the MZM modulator of Figure 2 is used for generating OSSB to reduce the influence of fiber dispersion. As for the optical fiber properties, the HNLF has an attenuation of 2.13 dB/km, a dispersion parameter of $-1.7 \cdot 10^{-12}$s^2/km and a fiber nonlinearity of 18 w^{-1}/km [38] and we rely on a 10 km DSF for signal transmission. In our design example we assume that each HNLF fiber has a length of 1 km.

Since the XPM- and SPM-induced phase-shifts fed into our four antenna elements is dependent both on the power level of the four control signals of the LD and on that of the data signals, we used the four optical attenuators of Figure 2 as the power controller for varying the power of each control signal having the same wavelengths to obtain the desired power. After the MZM, the quadruple-wavelength optical signal is demultiplexed, combined with each control signal and then fed into each HNLF. After transmitting through the HNLF and experiencing XPM-SPM-induced phase shift depending on the specific power level of both the modulated data signal and on that of each amplified control signal, we multiplex the output of the four HNLF and transmit the resultant WDM signal over a DSF, which exhibits zero dispersion in the wavelength region of 1550 nm.

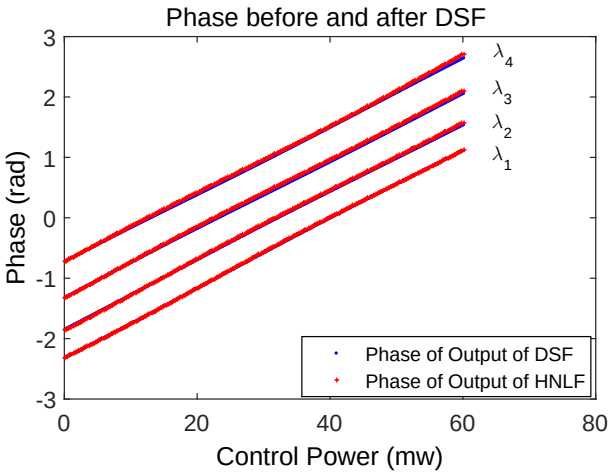


Figure 4: Attainable Phase Shifts of the 10 Gbps system.

In order to characterize the effect of each wavelength on the phase shift of the different signals, we fixed the input power for each wavelength to 0.1 milliWatt (mW) and varied the tunable power of the control signal from 0.1 mW to 60.1 mW with a step-size of 0.2 mW. Thus, the SPM maintains the same effect for each wavelength, implying that the phase-shift between each wavelength would only be affected by the XPM induced by the variation of the control signals' power. As a result, we obtained 301 power levels corresponding to the

Modulation Format	Quadrature Phase Shift Keying
Multi-wavelength	1549.4 (λ_4), 1549.6 (λ_3), 1549.8 (λ_2), 1550 (λ_1) nm (frequency spacing 25 GHz) Output Power of each Wavelength: 0.1 mW
Control Signal	1549.2 nm
Control Power Range (LD)	0.1 mW-60.1 mW
Optical Modulator	Dual-Drive MZM
HNLF Fiber Length	1 km
Dispersion-shifted Fiber Length	10 km
Bit rate	10 Gbps
RF Carrier Frequency	6 GHz
HNLF Attenuation	2.13 dB/km
HNLF Dispersion Parameter	$-1.7 \cdot 10^{-12}$ s^2/km
HNLF Fiber nonlinearity	18 w^{-1}/km

Table I: Simulation Parameters.

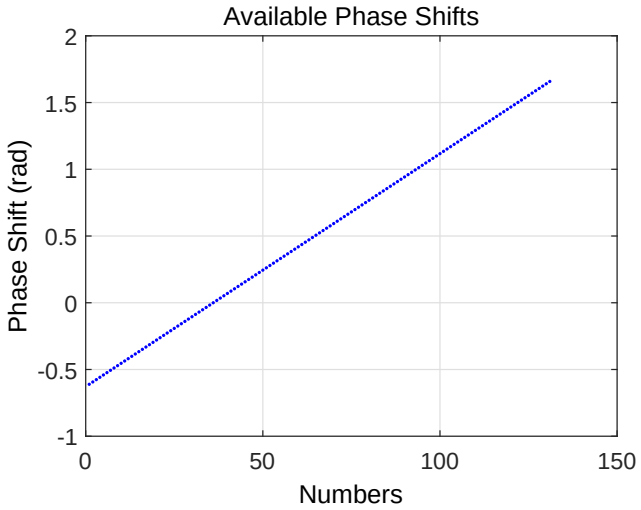


Figure 5: Attainable Phase Shifts of the 10 Gbps system.

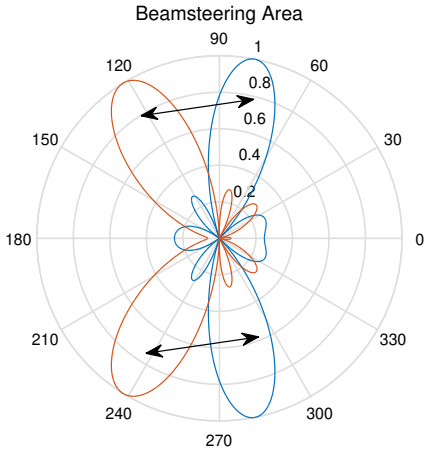


Figure 6: Beam Pattern of the 10 Gbps system.

four separate wavelengths. Then each optical wavelength was demodulated with the aid of coherent photodetection, yielding the photo-detected RF signal associated with a constant phase shift between the different photodetected RF signals. This was then translated into specific beamforming angles after being radiated from the PAA. Again, by collecting phase values corresponding to the above-mentioned power levels, we have attempted to identify the specific power for the particular optical wavelengths at which we have a constant phase shift between the four PAA elements. Furthermore, each control signal power associated with each wavelength can be tuned separately with the aid of four individual optical attenuators, thus granting us substantial flexibility, as shown in Figure 2.

To obtain a highly selective beamforming pattern, it is a challenge to maintain a constant phase shift between each and every element. As a solution, our design offers us a continuous phase tuning flexibility.

In our example, we used four parallel HNLFs to introduce phase shifts, while employing a DSF based techniques for transmitting the data to the RRHs. The measured phases of the four wavelengths at the outputs of both the HNLF and of the DSF are sketched in Figure 4, showing that they are nearly constant and hence indicating that our 10 km DSF only has a modest impact on the phase. Again, we can generate the required phase shifts based on the outputs of the parallel HNLF. Thus, we can simply test the parallel HNLFs and then design a codebook, storing the desired beamsteering directions and the corresponding level of the control powers required. Figure 5 shows the range of phase shifts available, which span from -0.6 rad to 1.6 rad[6]. As a result, Figure 6 portrays the corresponding angular directions, where a continuous scanning range of 90° is attained using a four-element PAA. Thus, we invoked our proposed system for cellular sectorization within a range below 90°, where a full range of 360° scanning angle is not required.

It was shown in [39] that having a phase error standard deviation for a four-element PAA system below 0.32 rad (18.33°) is suitable for guaranteeing a good beamforming performance. Based on the attainable phase shifts seen in Figure 5, we are able to keep the phase shift differences among the antenna elements within 0.01 rad, which may be deemed almost negligible. Hence our technique is capable of maintaining accurate directivity, outperforming the family of FBG techniques [35], [40], [41]. This is because the accuracy of the FBG family is determined by the fabrication imperfections of FBG, which potentially introduces group velocity ripples, hence potentially degrading the directivity accuracy.

[6]The x-axis in Figure 5 refers to the number of possible phase shifts that can be attained, with each corresponding to a specific control power combination.

Beamforming Direction	Power Combination (mWatt)				Phase shifts (rad)
	Power 1	Power 2	Power 3	Power 4	
80°	55.9	38.5	19.9	0.1	-0.54
85°	42.1	29.3	15.3	0.1	-0.28
90°	27.5	19.5	10.3	0.1	0
95°	13.3	9.9	5.1	0.1	0.28
100°	0.1	1.3	1.5	0.5	0.54
105°	0.1	6.1	11.1	15.5	0.82
110°	0.1	10.7	20.3	29.7	1.08
115°	0.1	14.9	29.3	42.9	1.33
120°	0.1	19.1	38.1	55.5	1.57

Table II: Power combinations required for obtaining different beamforming directions.

To briefly conclude the impact of XPM and SPM on the beamforming pattern, we extract specific power combinations corresponding to the beamsteering angles required for specific cell-sectorization angles. As explained in Section II-A1, the optical power induces fiber-nonlinearity, which can then cause the phase variation of each transmitted wavelength as verified by Equation (7). The phase variations are then exploited for obtaining a relationship between the optical power and the attainable constant phase shift of the adjacent antennas as portrayed by Figure 5, according to which we can form the specific beampattern of Figure 6. As an example, Table II shows some of the power combinations of the four control signal powers required for particular constant phase shifts for supporting the desired beam directions. These codebooks can be directly used by practitioners to design the sectorization patterns required.

1) Parametric study: As mentioned in Section II-A, the fiber impairments of SBS, SRS, FWM can be neglected, provided that we invoke SSFM for modelling the fiber-nonlinearity aided beamforming. Furthermore, there are other system parameters that affect our system performance and here we consider the MZM's nonlinearity, the optical input power and the HNLF length.

a) The MZM's nonlinearity: The MZM's nonlinearity is caused by the high amplitude of the MZM's drive voltage. As analyzed in [42], [43], the MZM's nonlinearity generates higher-order harmonics, which can potentially degrade our system performance. The MZM's modulation index (MI) $\frac{\pi V_{dr}}{V_\pi}$ determines the MZM's nonlinerity [42]. V_{dr} is the amplitude of the drive voltage of the MZM of Figure 2 and V_π is the switching voltage of the MZM. By controlling the amplitude V_{dr} to vary the modulation index according to 2.6, 3.7, 5.2 and 6.3, we obtained the output phase of the HNLF shown in Figure 7, while in the results reported in Figure 4, we fixed the MI to 0.5 to eliminate any harmonics. It is clearly shown that the phases obtained are fluctuated compared to the output phase of the HNLF seen in Figure 4 and the fluctuation becomes increasingly severe upon increasing the modulation index. In our proposed system, a MI of 0.5 is used for removing the second-order and higher-order side-bands caused by the MZM's nonlinearity.

b) The optical input power: In the performance study of Section III-A, we fixed the optical input power of the HNLF to 0.1 mW, which substantially reduced the SPM that might shift the phase in the transmitted DSF of Figure 2. To further characterise the impact of the optical input power, we vary the transmitted optical power according to 0.5, 1 and 2 mW and we compare the output phase of the HNLF and of the DSF of Figure 2. The results of Figure 8 indicate significant degradations when the power is increased to 2 mW, where the signal associated with the optical input power of 0.5 mW exhibits a similar performance to Figure 4 while the phase of two outputs divert marginally when the power is 1 mW. Thus, varying the optical input power for each wavelength feeding the HNLF will affect the corresponding beamforming direction instructed in the codebook shown in Table II.

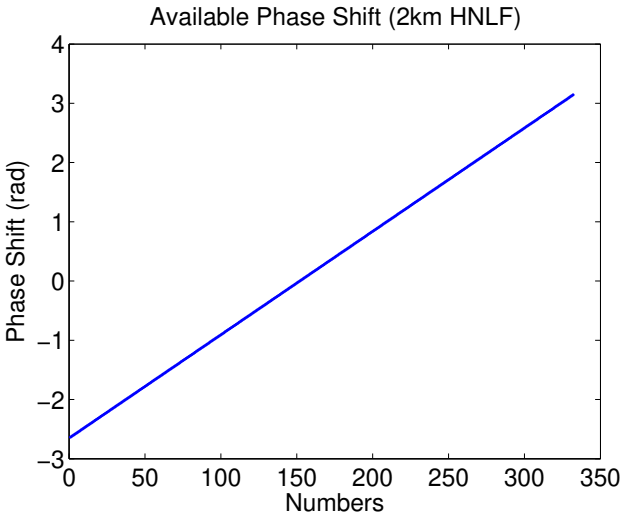


Figure 9: Attainable phase shifts with HNLFs fiber length of 2 km.

c) The HNLF fiber length: In our example, we proposed parallel HNLF fibers with each fiber length being 1 km for the sake of having a cost-efficient system design. However, we also noted that the achievable beamforming scanning range is limited to 90°. Thus, we increase our HNLF fiber length to 2 km to broaden the achievable range. Figure 9 shows that the achievable phase shifts have a range of -2.6 rad to π rad, implying that a beamforming scanning range of nearly 360° can be realized at the cost of having a longer fiber. Note that the longer fiber can be readily implemented by a cable drum, which can be accommodated without requiring larger space. Alternatively, a highly nonlinear chalcogenide fiber having a nonlinearity of 50,000 times that of the standard silica fiber [44] can also be used in our system for the sake of reducing the overall fiber length to a few meters.

The above-mentioned parameters are likely to affect the RoF system and should be carefully tailored. Since our system is designed for cellular sectorization, a beamforming scanning angle within 90° is satisfactory. Our C-RAN application is based on the codebook given by Table II designed for cellular sectorization.

B. C-RAN BER Performance

We have indicated in Section I and II-A that our system is capable of simplifying the electronic phase-shifter based conventional beamforming transceiver system implemented in the conventional base station by beneficially exploiting the fiber-nonlinearity aided beamforming technique. C-RAN is widely recognized as a cost- and energy-efficient mobile access network for reducing the Total Cost of Ownership (TCO) [8], such as the management and maintenance fee, by

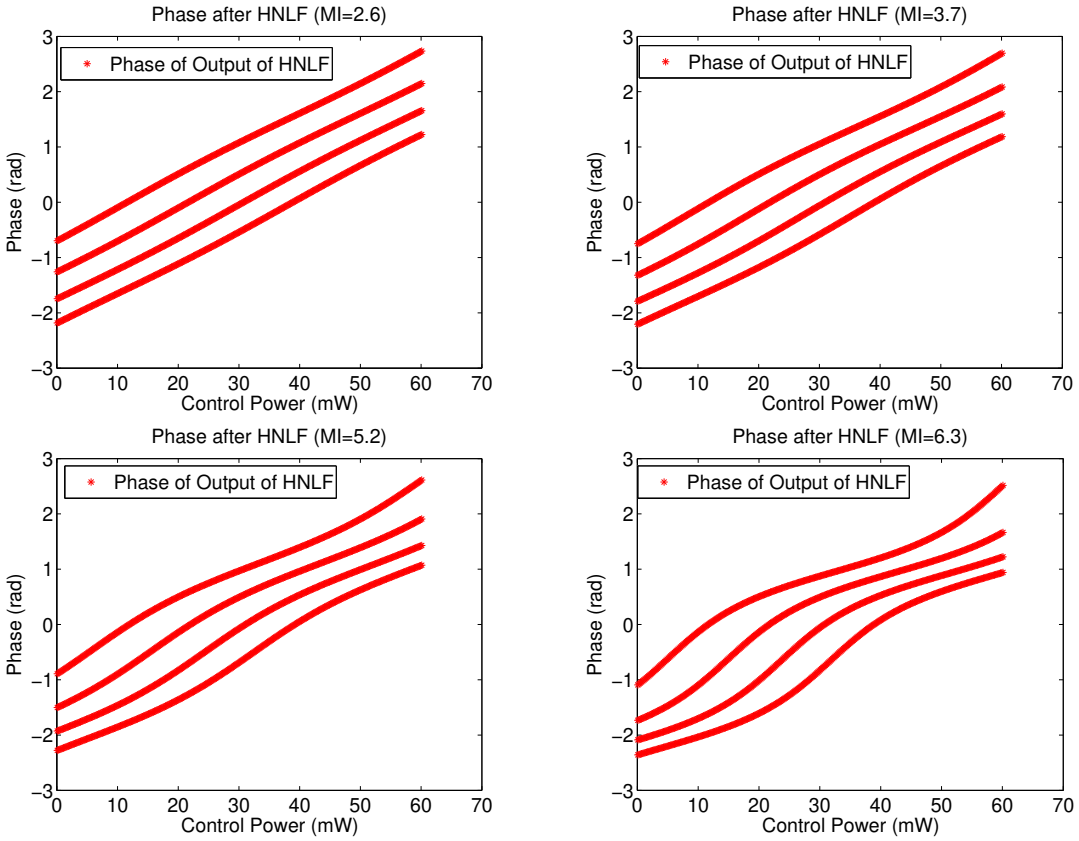


Figure 7: Output phase of HNLF with various MI.

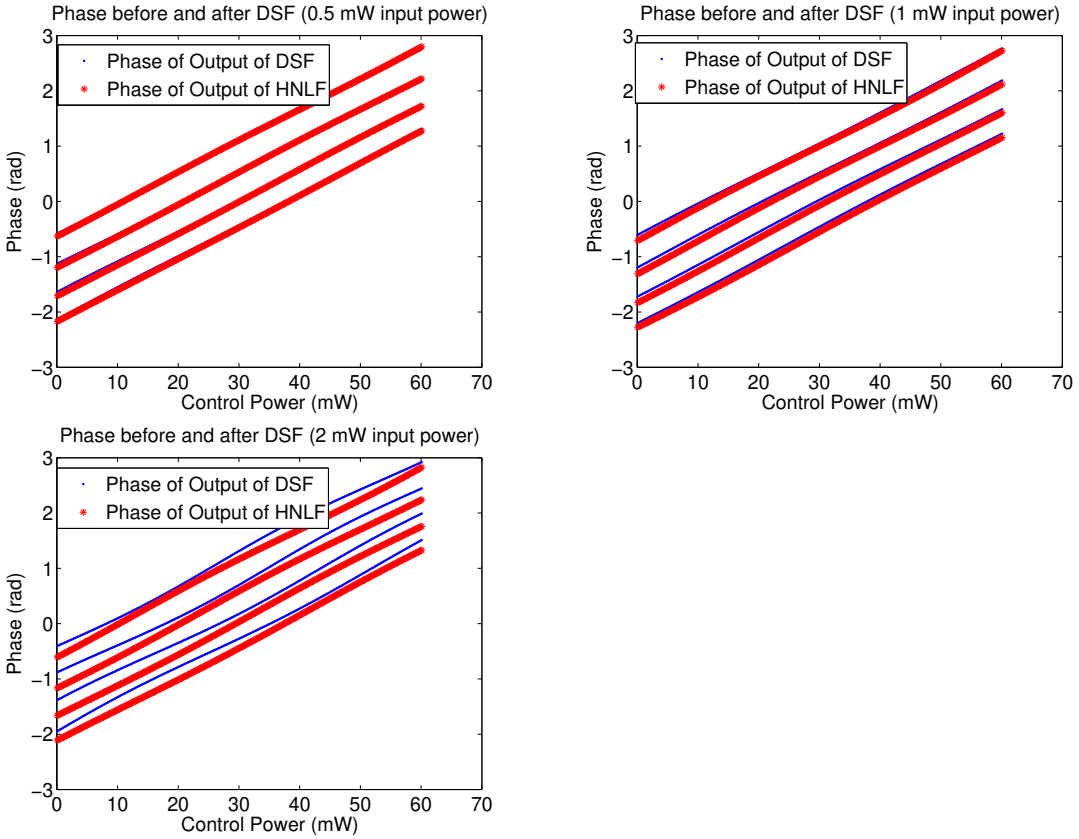


Figure 8: Output phase before and after the DSF with various input optical power.

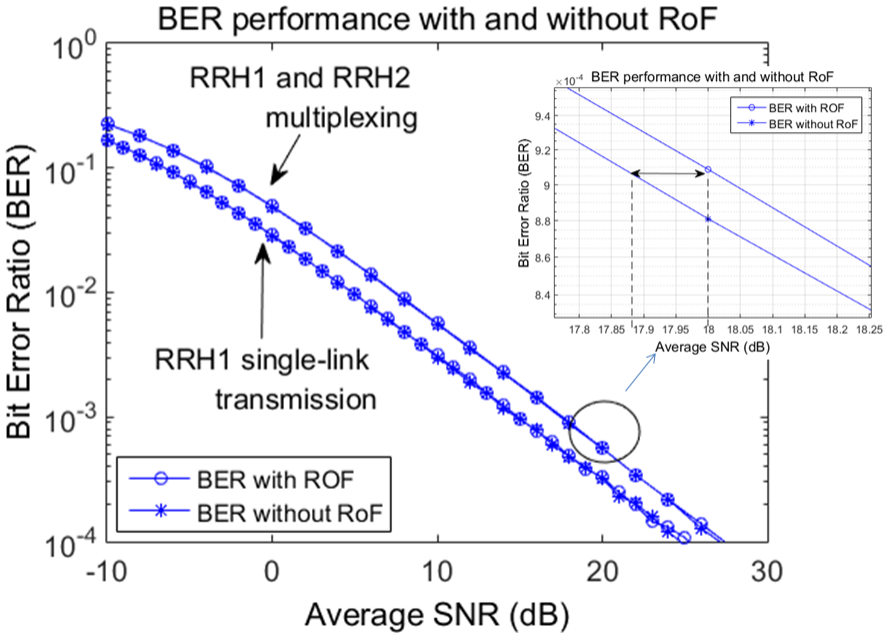


Figure 10: BER performance with and without RoF.

centralizing most of the digital signal processing in a central office. More specifically, regarding the analogue beamforming system design, we centralize the beamforming pattern control in the central office, while exploiting fiber nonlinearity to shape the phase response. Hence we eliminate the need for the analogue phase shifters. For example, as discussed in [12], the number of electronic phase-shifters of a conventional analogue beamforming system is a linear function of the number of transmitter antennas. Thus, a four-transmitter-antenna aided beamforming system requires four RF phase shifters and four RF chains, which are housed in the RRHs. In the proposed fiber-nonlinearity aided beamforming system, actively powered phase shifters, power-thirsty analogue-to-digital converter (ADC) and digital-to-analogue converters (DAC) are totally eliminated, while invoking four short HNLFs of 1 km length in the central office to obtain the designed beamforming phase response. The beamforming angle control is confined to the central office, where the complexity of the conventional base station imposed by the beamforming is substantially reduced. Furthermore, the central office is capable of steering the beam transmitted from multiple RRHs, which will be discussed in this section.

Since the codebook of Table II can be used for generating specific beams, the centrally power-controlled beam steering scheme is capable of supporting our C-RAN system, which relies on low-complexity RRHs. Here, to validate that our proposed system can be exploited in a C-RAN system, we have discussed the amalgamation of RoF and C-RAN in Section II-A2. The associated performance results are presented in this section. Based on the C-RAN system of Figure 3 and on the discussions of Section II-A2, the UE of Figure 3 can be connected either only to RRH1 or to both RRH1 and RRH2, depending on the prevalent channel conditions as detailed in Section II-A2. We consider both cases and show the bit error ratio (BER) performance attained in Figure 10.

Figure 10 shows the BER performance of the fiber aided beamformer and of the beamformer using conventional phase-shifters without RoF as a bench marker. As discussed in [29], when one of the RRHs of Figure 3 is in deep fade, the C-RAN system is capable of switching to another RRH (e.g. RRH1 of Figure 3) for transmission. The corresponding BER curve of the single-link RRH1 is shown in Figure 10, which shows only modestly degraded BER results compared to those using conventional electronic phase-shifters without RoF[7].

On the other hand, when the UE is connected to both RRH1 and RRH2[8], two independently fading spatial streams are transmitted to the user positioned at angle 105° and 120° from RRH1 and RRH2 of Figure 3 invoked for spatial multiplexing, respectively [45]. It can be seen from Figure 10 that the fiber aided beamformer shows a negligible 0.1 dB SNR degradation compared to that of the beam steering using conventional phase-shifters without RoF. This is due to the phase noise introduced by RoF system. Furthermore, due to the interference introduced by multiplexing shown in Figure 10, we achieved a better performance for the RRH1-based single-link transmission than that for multiplexing. Thus, as evidenced by Figure 10, our RoF aided beamforming technique is capable of supporting a C-RAN system, whilst reducing the cost- and energy-consumption compared to the conventional electronic phase-shifter aided beamforming system.

[7]The SNR in Figure 10 represents the wireless SNR, where the measured signal power is the normalized output power of the PAAs and the noise power is the wireless AWGN power.

[8]Again, as mentioned in Section III-A1c, using a longer fiber or a fiber with higher nonlinearity factor, it is possible to extend the coverage angle of the antenna array in each RRH to 360°. In this example, where the coverage angle is 90°, it is possible to employ four antenna arrays at the same RRH, where each antenna array can cover a different 90° area and hence the RRH will be able to cover the entire 360° area.

Hence our solution may be readily invoked for sectorization of a C-RAN cellular network to improve the SNR gain attained.

IV. Conclusions

In this paper, a novel phase shifting network relying on fiber nonlinearity has been proposed for analogue wireless beamforming, which was investigated in the context of a C-RAN system. Explicitly, the optical power-dependent phase information has been translated into a particular beam-steering pattern using our RoF design. It was shown that the beamforming angles may be configured to cover a range of about 90°. Our system can be centrally controlled using our novel HNLF aided tunable beamforming scheme, which can also be utilized for the C-RAN fronthaul. Furthermore, a 10 Gbps QPSK signal transmitted in the downlink of a C-RAN system implementing our HNLF aided beamforming scheme was characterized, where the BER performance shows only a modest degradation compared to that using additionally conventional electronic phase-shifters. Furthermore, future work can be focused on the C-RAN's response time and sum-rate, as addressed [46].

References

[1] L. Hanzo, H. Haas, S. Imre, D. O'Brien, M. Rupp, and L. Gyongyosi, "Wireless myths, realities, and futures: From 3G/4G to optical and quantum wireless," *Proceedings of the IEEE*, vol. 100, pp. 1853–1888, May 2012.

[2] W. Roh, "5g mobile communications for 2020 and beyond-vision and key enabling technologies," *Samsung Electronics Corporate*, 2014.

[3] H. Subbaraman, M. Y. Chen, and R. T. Chen, "Photonic crystal fiber-based true-time-delay beamformer for multiple RF beam transmission and reception of an X-band phased-array antenna," *Journal of Lightwave Technology*, vol. 26, pp. 2803–2809, Aug. 2008.

[4] J. Andrews, S. Buzzi, W. Choi, S. Hanly, A. Lozano, A. Soong, and J. Zhang, "What will 5G be?," *IEEE Journal on Selected Areas in Communications*, vol. 32, pp. 1065–1082, June 2014.

[5] M. Peng, K. Zhang, J. Jiang, J. Wang, and W. Wang, "Energy-efficient resource assignment and power allocation in heterogeneous cloud radio access networks," *IEEE Transactions on Vehicular Technology*, vol. 64, pp. 5275–5287, Nov. 2015.

[6] V. N. Ha, L. B. Le, and N. D. Dao, "Coordinated multipoint transmission design for cloud RANs with limited fronthaul capacity constraints," *IEEE Transactions on Vehicular Technology*, vol. 65, pp. 7432–7447, Sept. 2016.

[7] M. Peng, C. Wang, V. Lau, and H. V. Poor, "Fronthaul-constrained cloud radio access networks: Insights and challenges," *IEEE Wireless Communications*, vol. 22, pp. 152–160, April 2015.

[8] A. Checko, H. L. Christiansen, Y. Yan, L. Scolari, G. Kardaras, M. S. Berger, and L. Dittmann, "Cloud RAN for mobile networks-a technology overview," *IEEE Communications Surveys and Tutorials*, vol. 17, no. 1, pp. 405–426, 2015.

[9] Y. Li, M. El-Hajjar, and L. Hanzo, "Joint space-time block-coding and beamforming for the multi-user radio over plastic fiber downlink," *IEEE Transactions on Vehicular Technology*, vol. PP, no. 99, pp. 1–1, 2017.

[10] R. A. Minasian and K. E. Alameh, "Optical-fiber grating-based beamforming network for microwave phased arrays," *IEEE Transaction on Microwave Theory and Techniques*, vol. 45, pp. 1513–1518, Aug. 1997.

[11] L. Xu, R. Taylor, and S. R. Forrest, "The use of optically coherent detection techniques for true-time delay phased array and systems," *Journal of Lightwave Technology*, vol. 13, pp. 1663–1678, Aug. 1995.

[12] Z. Cao, Q. Ma, A. B. Smolders, Y. Jiao, M. J. Wale, C. W. Oh, H. Wu, and A. M. J. Koonen, "Advanced integration techniques on broadband millimeter-wave beam steering for 5G wireless networks and beyond," *IEEE Journal of Quantum Electronics*, vol. 52, pp. 1–20, Jan. 2016.

[13] A. Molony, L. Zhang, J. Willlams, I. Bennion, C. Edge, and J. Fells, "Fiber Bragg grating networks for time-delay control of phased-array antennas," in *Summaries of papers presented at the 1996 Conference on Lasers and Electro-Optics*, pp. 244–245, IEEE, June 1996.

[14] G. A. Ball, W. Glenn, and W. Morey, "Programmable fiber optic delay line," *IEEE Photonics Technology Letters*, vol. 6, pp. 741–743, June 1994.

[15] B. Ortega, J. L. Cruz, J. Capmany, M. V. Andrés, and D. Pastor, "Analysis of a microwave time delay line based on a perturbed uniform fiber Bragg grating operating at constant wavelength," *Journal of Lightwave Technology*, vol. 18, pp. 430–436, March 2000.

[16] D. B. Hunter, M. E. Parker, and J. L. Dexter, "Demonstration of a continuously variable true-time delay beamformer using a multichannel chirped fiber grating," *IEEE Transaction on Microwave Theory and Techniques*, vol. 54, pp. 861–867, Feb. 2006.

[17] J. Yao, J. Yang, and Y. Liu, "Continuous true-time-delay beamforming employing a multiwavelength tunable fiber laser source," *IEEE Photonics Technology Letters*, vol. 14, no. 5, pp. 687–689, 2002.

[18] Y. Liu, J. Yang, and J. Yao, "Continuous true-time-delay beamforming for phased array antenna using a tunable chirped fiber grating delay line," *IEEE Photonics Technology Letters*, vol. 14, no. 8, pp. 1172–1174, 2002.

[19] R. Bonjour, S. A. Gebrewold, D. Hillerkuss, C. Hafner, and J. Leuthold, "Ultra-fast tunable true-time delay using complementary phase-shifted spectra (CPSS)," in *2015 Optical Fiber Communication Conference*, p. W2A.67, Optical Society of America, March 2015.

[20] O. Raz, S. Barzilay, R. Rotman, and M. Tur, "Fast switching and wide-band photonic beamformer with flat RF response and squintless scan performance," in *2007 Conference on Optical Fiber Communication and the National Fiber Optic Engineers Conference*, pp. 1–3, March 2007.

[21] V. S. Ilchenko and A. B. Matsko, "Optical resonators with whispering-gallery modes-Part II: applications," *IEEE Journal of Selected Topics in Quantum Electronics*, vol. 12, pp. 15–32, Jan. 2006.

[22] T. Mengual, B. Vidal Rodriguez, C. Stoltidou, S. Blanch, J. Martí, L. Jofre, I. McKenzie, and J. M. Del Cura, "Optical beamforming network with multibeam capability based on a spatial light modulator," in *2008 Optical Fiber Communication Conference*, p. JThA71, Optical Society of America, Feb. 2008.

[23] P. Q. Thai, A. Alphones, and D. R. Lim, "Limitations by group delay ripple on optical beam-forming with chirped fiber grating," *Journal of Lightwave Technology*, vol. 27, pp. 5619–5625, Dec. 2009.

[24] M. Hirano, T. Nakanishi, T. Okuno, and M. Onishi, "Silica-based highly nonlinear fibers and their application," *IEEE Journal of Selected Topics in Quantum Electronics*, vol. 15, pp. 103–113, Jan. 2009.

[25] A. Loayssa, S. Galech, and F. Lahoz, "Broadband microwave photonic phase-shifter based on stimulated Brillouin scattering," in *The 18th Annual Meeting of the IEEE Lasers and Electro-Optics Society*, pp. 839–840, Oct. 2005.

[26] Y. Dong, H. He, W. Hu, Z. Li, Q. Wang, W. Kuang, T. H. Cheng, Y. J. Wen, Y. Wang, and C. Lu, "Photonic microwave phase shifter/modulator based on a nonlinear optical loop mirror incorporating a Mach-Zehnder interferometer," *Optics Letters*, vol. 32, pp. 745–747, April 2007.

[27] W. Li, W. H. Sun, W. T. Wang, and N. H. Zhu, "Optically controlled microwave phase shifter based on nonlinear polarization rotation in a highly nonlinear fiber," *Optics Letters*, vol. 39, pp. 3290–3293, June 2014.

[28] G. P. Agrawal, *Fiber-optic communication systems*, vol. 222. John Wiley & Sons, 2012.

[29] K. Satyanarayana, M. El-Hajjar, P. H. Kuo, A. Mourad, and L. Hanzo, "Adaptive transceiver design for C-RAN in mmwave communications," *IEEE Access*, vol. PP, pp. 1–1, Nov. 2017.

[30] T. S. Rappaport, *Wireless communications: principles and practice*, vol. 2. prentice hall PTR New Jersey, 1996.

[31] G. P. Agrawal, *Nonlinear fiber optics*. Academic press, 2007.

[32] G. P. Agrawal, "Nonlinear fiber optics: its history and recent progress," *JOSA B*, vol. 28, pp. A1–A10, Dec. 2011.

[33] J. Leibrich and W. Rosenkranz, "Efficient numerical simulation of multichannel WDM transmission systems limited by XPM," *IEEE Photonics Technology Letters*, vol. 15, pp. 395–397, March 2003.

[34] C. A. Balanis, *Antenna theory: analysis and design*, vol. 1. John Wiley & Sons, 2005.

[35] S. Blais and J. Yao, "Photonic true-time delay beamforming based on superstructured fiber Bragg gratings with linearly increasing equivalent chirps," *Journal of Lightwave Technology*, vol. 27, pp. 1147–1154, May 2009.

[36] M. Hirano, T. Nakanishi, T. Okuno, and M. Onishi, "Silica-based highly nonlinear fibers and their application," *IEEE Journal of Selected Topics in Quantum Electronics*, vol. 15, pp. 103–113, Jan. 2009.

[37] K. Satyanarayana, M. El-Hajjar, P. H. Kuo, A. Mourad, and L. Hanzo, "Dual-function hybrid beamforming and transmit diversity aided millimeter wave architecture," *IEEE Transactions on Vehicular Technology*, vol. PP, pp. 1–1, March 2017.

[38] L. Provost, C. Finot, K. Mukasa, P. Petropoulos, and D. J. Richardson, "Generalisation and experimental validation of design rules for self-phase modulation-based 2R-regenerators," in *2007 Optical Fiber Communication Conference and Exposition and The National Fiber Optic Engineers*, pp. 1–3, Optical Society of America, March 2007.

[39] B. Peng, S. Priebe, and T. Kurner, "Effects of phase shift errors on the antenna directivity of phased arrays in indoor terahertz communications," in *2014 11th International Symposium on Wireless Communications Systems (ISWCS)*, pp. 355–359, Aug. 2014.
[40] J. Corral, J. Marti, and J. Fuster, "Optical beamforming network based on chirped fiber gratings continuously variable true-time-delay lines," in *1998 IEEE MTT-S International Microwave Symposium Digest*, vol. 3, pp. 1379–1382, IEEE, June 1998.
[41] F. Zeng, J. Yao, and T. Yeap, "Dispersion effects and implementation errors on uniform fiber Bragg grating based true-time-delay beamforming networks," in *Proceedings of the 2003 International Topical Meeting on Microwave Photonics*, pp. 337–340, Sept. 2003.
[42] M. Mohamed, X. Zhang, B. Hraimel, and K. Wu, "Analysis of frequency quadrupling using a single Mach-Zehnder modulator for millimeter-wave generation and distribution over fiber systems," *Optics Express*, vol. 16, pp. 10786–10802, July 2008.
[43] V. Thomas, M. El-Hajjar, and L. Hanzo, "Performance improvement and cost reduction techniques for radio over fiber communications," *IEEE Communications Surveys Tutorials*, vol. 17, pp. 627–670, Second Quarter 2015.
[44] D.-I. Yeom, E. C. Magi, M. R. Lamont, L. Fu, and B. J. Eggleton, "Low-threshold supercontinuum generation in dispersion engineered highly nonlinear chalcogenide fiber nanowires," in *2008 Conference on Optical Fiber communication/National Fiber Optic Engineers*, pp. 1–3, IEEE, March 2008.
[45] V. A. Thomas, M. El-Hajjar, and L. Hanzo, "Single ODSB radio-over-fiber signal supports STBC at each RAP," *IEEE Communications Letters*, vol. 19, pp. 1331–1334, May 2015.
[46] H. Ren, N. Liu, C. Pan, M. Elkashlan, A. Nallanathan, X. You, and L. Hanzo, "Low-latency C-RAN: An next-generation wireless approach," *IEEE Vehicular Technology Magazine*, vol. 13, pp. 48–56, June 2018.



Yichuan Li received B.Sc. degree in Optics Information Science and Technology from China University of Petroleum (East China), Qingdao, China, in 2012, and M.Sc. degree in wireless communications from the University of Southampton, Southampton, UK., in 2014. He was a research assistant in the Lightwave Communication Lab of the Chinese University of Hong Kong (CUHK) from July to October in 2017. Currently, he is working toward the Ph.D. degree with the University of Southampton. His research is focused on the the radio over fiber for backhaul, fronthaul and indoor communication network. His research interests are millimeter wave over fiber, optical fiber aided analogue beamforming techniques, Multifunctional MIMO, mode division multiplexing in multimode fiber and fiber-based C-RAN system.



Dr. Salman Ghafoor received BSc Electrical Engineering degree from UET Peshawar, Pakistan in 2006. In 2007, he received MSc degree in Electronic Communications and Computer Engineering from University of Nottingham, UK. Dr. Salman worked for 2 years as a research student at the Optoelectronics Research Centre (ORC), University of Southampton, UK. In 2010, Dr. Salman joined the School of Electronics and Computer Science (ECS), University of Southampton where he completed his PhD degree in 2012. Currently Dr Salman is working as an assistant professor at NUST, Pakistan. His areas of research are All-optical signal processing, Ultra-wideband over Fibre and Radio over Fibre systems.



Katla Satyanarayana (http://www.satyanarayana.xyz) received his B. Tech. degree in Electrical Engineering from Indian Institute of Technology Madras, India, in 2014. During Jul'14-Aug'15, he worked as a research assistant at Indian Institute of Science, Bangalore. Currently, Satya is a research scholar in Wireless Communications at the University of Southampton in liaison with InterDigital Europe, London, UK. His research interests include millimeter wave communications, hybrid beamforming, with an emphasis on transceiver algorithms for wireless communication systems and multi-functional MIMO.



Mohammed El-Hajjar is an Associate Professor in the Department of Electronics and Computer Science in the University of Southampton. He received his PhD in Wireless Communications from the University of Southampton, UK in 2008. Following the PhD, he joined Imagination Technologies as a design engineer, where he worked on designing and developing Imagination's multi-standard communications platform, which resulted in three patents. He is the recipient of several academic awards and has published a Wiley-IEEE book and in excess of 80 journal and conference papers. Mohammed's research interests include the development of intelligent communications systems, energy-efficient transceiver design, MIMO, millimeter wave communications and Radio over fiber network design.



Lajos Hanzo (http://www-mobile.ecs.soton.ac.uk) FREng, FIEEE, FIET, Fellow of EURASIP, DSc received his degree in electronics in 1976 and his doctorate in 1983. In 2009 he was awarded an honorary doctorate by the Technical University of Budapest and in 2015 by the University of Edinburgh. In 2016 he was admitted to the Hungarian Academy of Science. During his 40-year career in telecommunications he has held various research and academic posts in Hungary, Germany and the UK. Since 1986 he has been with the School of Electronics and Computer Science, University of Southampton, UK, where he holds the chair in telecommunications. He has successfully supervised 112 PhD students, co-authored 18 John Wiley/IEEE Press books on mobile radio communications totalling in excess of 10 000 pages, published 1800+ research contributions at IEEE Xplore, acted both as TPC and General Chair of IEEE conferences, presented keynote lectures and has been awarded a number of distinctions. Currently he is directing an academic research team, working on a range of research projects in the field of wireless multimedia communications sponsored by industry, the Engineering and Physical Sciences Research Council (EPSRC) UK, the European Research Council's Advanced Fellow Grant and the Royal Society's Wolfson Research Merit Award. He is an enthusiastic supporter of industrial and academic liaison and he offers a range of industrial courses. He is also a Governor of the IEEE ComSoc and VTS. During 2008 - 2012 he was the Editor-in-Chief of the IEEE Press and a Chaired Professor also at Tsinghua University, Beijing. For further information on research in progress and associated publications please refer to http://www-mobile.ecs.soton.ac.uk.